A closed form solution for a three dimensional passive earth pressure coefficient

Ernesto Motta,* Erminia Raciti*

Summary

Estimation of passive pressure under both static and seismic conditions is very important for the design of diaphragm walls, anchors, foundations etc. It has been shown in technical literature that in case of limited width of the "plate" on which earth pressure acts, the influence of the third dimension can be significant, due to side effects so that the three-dimensional passive earth pressure coefficient is greater than the two-dimensional one. Unfortunately, no closed form solution for the evaluation of this coefficient is available till now, but only results listed in tables or shown in plots versus B/H ratios, being B and H the plate width and height, respectively.

In this work, an extension of the classical Mononobe-Okabe-Kapila method is presented and a closed form solution for the evaluation of three-dimensional passive earth pressure coefficient is obtained and applied. Similarly to numerical approaches in literature, the proposed solution takes into account the friction angle of the soil and that of the soil-plate interface while, as a novelty, it allows to take into account the slope angle of the backfill, and seismic actions through a pseudo-static approach. The model is validated in static conditions, by comparisons with solutions obtained by other authors through different approaches.

1. Introduction

As known, passive earth pressure is the limit resistance of a soil mass against the displacement caused by a forcing structural element. Evaluating this pressure is of significant practical importance in dealing with the design of diaphragm walls, anchors, foundations, etc. Coulomb [1773] applying the limit equilibrium method, was the first who studied the problem of lateral earth pressure on retaining structures. About one century later, Rankine [1857] developed the simplest procedure for computing minimum active and maximum passive earth pressures. Referring to passive earth pressure, most researchers concentrated their efforts in refining two-dimensional analyses, in static or in seismic conditions, presenting models based or on limit-equilibrium method [Kapila, 1962; Shields and Tolunay, 1972; 1973; Rahardjo and Fredlund, 1984; Zakerzadeh *et al.*, 1999; Subba Rao and Choudhury, 2005], or on slip line method [Caquot and Kerisel, 1949; Sokolovski, 1960], or on limit analysis methods [Lysmer, 1970; Lee and Herington, 1972; Chen and Rosenfarb, 1973; Soubra, 2000; Lancellotta, 2002; 2007]. Even if the limit equilibrium method gives only approximate results, it allows to obtain closed form solutions, widely applied in professional practice. One example is the Coulomb derived Mononobe-Okabe-Kapila method [Kapila, 1962] for the evaluation of a two-dimensional passive earth pressure coefficient both in static and in seismic conditions.

However, it cannot be neglected that there are several geotechnical structures, such as anchor blocks, anchor plates, diaphragm walls and so on, in which three-dimensional (3D) effects are quite evident. Three-dimensional solutions for passive earth pressure were presented by Blum [1932] using the limit equilibrium method, by Soubra and Regenass [2000] using the limit analysis with a multi-block translation failure mechanism, by Škrabl and Macuh [2008] using a rotational hyperbolical failure mechanism and by Vrecl-Kojc and Škrabl [2007] by the upper bound theorem within the framework of the limit analysis. Numerical models based on Finite Difference Method (FDM) were presented by Benmebarek *et al.* [2008] and Benmeddour *et al.* [2010].

Models investigating three-dimensional passive earth pressure on a plate, of width *B* and height *H*, have been usually solved by numerical approaches thus they do not give closed form solutions. The obtained results are listed in tables or shown in plots, in terms of 3D passive earth pressure coefficient values versus *B/H* ratios. Moreover, none of these analyses takes into account seismic effects and/or slope inclination, so they cannot be applied in most real cases for a seismic design.

Limit equilibrium models based on Coulomb failure wedge allowed to obtain closed form solutions in many practical cases concerning two-dimensional or three-dimensional active earth pressure problems [Motta, 1993; Motta, 2012]. In this work, an extension of the classical Mononobe-Okabe-Kapila method is presented and a closed form solution for the evaluation of three-dimensional passive earth pressure coefficient is obtained and applied. Like numerical approaches available in literature, the proposed method allows to take into account the soil friction angle and the soil-wall interface friction angle. Moreover, as a novelty, the influence of the

* Department of Civil Engineering and Architecture, University of Catania

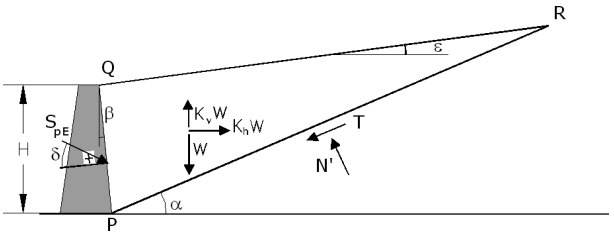

Fig. 1 – KAPILA [1962] model for the analysis of passive earth pressure in pseudo-static conditions.
Fig. 1 – Modello di KAPILA [1962] per l'analisi della spinta passiva in condizioni pseudo-statiche.

slope of the soil mass, and that of the seismic coefficients for a pseudo-static analysis can be studied with this approach. Some results concerning different values of slope angles and seismic coefficients, will be presented in terms of seismic three-dimensional passive earth pressure coefficient values.

2. The Mononobe-Okabe-Kapila method

As widely known, in the 1920s, OKABE [1926] and MONONOBE and MATSUO [1929] developed from the COULOMB [1773] wedge theory the MONONOBE-OKABE method, useful to evaluate the active earth pressure coefficient taking into account, in a pseudo-static approach, the vertical and horizontal acceleration induced by an earthquake. KAPILA [1962] modified the MONONOBE-OKABE method to consider passive earth pressure conditions. The obtained expression for the total passive force is a straightforward extension of the COULOMB sliding wedge theory for incorporating the pseudo-static horizontal and vertical inertial forces caused by earthquakes, so it is known as MONONOBE-OKABE-KAPILA method.

According to MONONOBE-OKABE-KAPILA method, the seismic passive thrust for a unit width of wall in a dry cohesionless soil is given by:

$$S_{pE}=\frac{1}{2}\gamma\cdot H^2\cdot K_{pE}\cdot(1-K_v) \qquad (1)$$

where γ is the soil unit weight, H is the height of the soil where S_{PE} is acting, K_v, is the vertical seismic coefficient and K_{PE} is the dynamic passive earth pressure coefficient given by:

$$K_{pE}=\frac{\cos^2(\varphi'+\beta-\theta)}{\cos\theta\cdot\cos^2\beta\cdot\cos(\delta-\beta-\theta)\cdot\left[1-\sqrt{\frac{\sin(\delta+\varphi')\cdot\sin(\varphi'+\varepsilon-\theta)}{\cos(\delta-\beta+\theta)\cdot\cos(\varepsilon-\beta)}}\right]^2} \qquad (2)$$

where β is the inclination of the plate interior side, ε is the backfill slope angle, φ' is the soil friction angle, δ is the soil –plate interface friction angle and θ is the seismic angle, given by:

$$\theta=\tan^{-1}\left[\frac{K_h}{1-K_v}\right] \qquad (3)$$

being K_h and K_v the horizontal and vertical seismic coefficient respectively K_v is assumed positive if the material vertical faces act upwards.

The critical failure surface in the KAPILA solution is inclined from the horizontal by an angle:

$$\alpha_{PE}=\theta-\varphi'+\tan^{-1}\left[\frac{-\tan(\varphi'+\theta+\varepsilon)+C_1}{C_2}\right] \qquad (4)$$

where:

$$C_1=\sqrt{\tan(\varphi'-\theta+\varepsilon)\cdot[\tan(\varphi'-\theta+\varepsilon)+\cot(\varphi'-\theta+\beta)]}\cdot \cdot\sqrt{1+\tan(\delta-\theta+\beta)\cdot\cot(\varphi'-\theta+\beta)} \qquad (5)$$

$$C_2=1+\{\tan(\delta+\theta-\beta)\cdot[\tan(\varphi'-\theta+\varepsilon)+\cot(\varphi'-\theta+\beta)]\} \qquad (6)$$

There are some limitations in using MONONOBE-OKABE-KAPILA formula. In fact it is known that COULOMB theory in the passive case gives results in good agreement with more sophisticated approaches only when the soil-wall interface angle, δ, is low; otherwise it overestimates the passive earth pressure coefficient, giving results on the unsafe side. For example, in table I a comparison between passive earth pressure coefficient by KAPILA [1962] for the static case (θ=0), using the planar failure surface, and by SOUBRA and REGENASS [2000], using a log-spiral failure surface in the strip foundation case, shows that, the greater is the soil-wall friction angle, the greater is the scatter between the two passive earth pressure coefficients considered. Moreover the greater is the soil friction angle, the greater is the scatter. In all these cases KAPILA coefficient is or on the unsafe side

Tab. I – Comparison between passive earth pressure coefficient by KAPILA [1962] and by SOUBRA E REGENASS [2000].
Tab. I – Confronto fra il coefficiente di spinta passiva determinato con la formula di KAPILA [1962], e quello dedotto da SOUBRA E REGENASS [2000].

φ	δ/φ	Passive earth pressure coefficient (static case)		scatter [%]
		Kapila [1962]	Soubra and Regenass [2000] (strip foundation case)	
15	0	1.70	1.70	0.0
15	0.5	2.01	1.99	1.2
15	1	2.40	2.25	6.7
20	0	2.04	2.04	0.0
20	0.5	2.65	2.58	2.9
20	1	3.52	3.13	12.6
30	0	3.00	3.00	0.0
30	0.5	4.98	4.69	6.1
30	1	10.10	6.91	46.2
40	0	4.60	4.60	0.0
40	0.5	11.77	9.99	17.8
40	1	92.58	19.94	364.3

with respect to SOUBRA and REGENASS [2000] coefficient or it is equal, if $\delta/\varphi = 0$.

3. Extension of the Mononobe-Okabe-Kapila method for a three-dimensional passive earth pressure coefficient

Let us consider a rigid vertical plate, PP'Q'Q acting against a dry cohesionless soil as shown in figure 2. Limit equilibrium is assumed to be reached due to the force S_{p3D} applied on the plate. Because of the structure limited width, a three dimensional passive limit state is attained. In this case three-dimensional effects can be taken into account by modifying the conceptually simple, previously described, KAPILA formula according to the model shown in figure 2. The following assumptions have been made in the analysis:

- the soil is homogeneous and cohesionless;
- the plate, of dimensions B x H (B = width; H = height), is vertical ($\beta = 0$);
- the lower slip surface is planar and inclined to the horizontal direction of an angle α;
- the backfill is planar and inclined to the horizontal direction of an angle ε;
- the geometry of the soil wedge and the forces acting on it do not change along the base B direction;
- a translational movement is considered, that is the soil wedge slides along the base surface PP' R'R and along the lateral surfaces PQR and P'Q'Q', on which of them a resistance T_L acts (see figure 2).

Let us assume:

- T_B the resultant of the total resistance acting along the base of the failure wedge;
- T_L the resultant of the lateral boundary total resistance acting on each side of the failure wedge
- η the angle between the direction of T_L and the horizontal direction.

Based on whole wedge equilibrium along the horizontal and vertical directions and taking into account seismic loading, one can write:

$$S_{p3D}\cdot\cos\delta - T_B\cdot\cos\alpha - N'\cdot\sin\alpha + K_h\cdot W - 2\cdot T_L\cdot\cos\eta = 0 \quad (7)$$

$$W\cdot(1-K_v) + S_{p3D}\cdot\sin\delta + T_B\cdot\sin\alpha - N'\cdot\cos\alpha + 2\,T_L\cdot\sin\eta = 0 \quad (8)$$

Furthermore, if limit equilibrium is reached along the base, the following equation can be written:

$$T_B = N'\cdot\tan\varphi' \quad (9)$$

The soil weight W can be evaluated by simple geometrical considerations while the two lateral resistance, T_L, can be determined by the following integral:

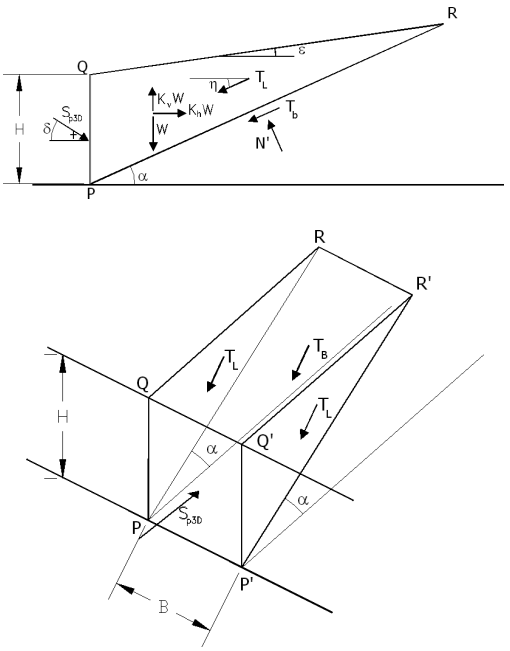

Fig. 2 – Three-dimensional model for the analysis of passive earth pressure coefficient; a) cross section; b) Three-dimensional view.
Fig. 2 – Modello tridimensionale per l'analisi del coefficiente di spinta passiva; a) sezione trasversale; b) vista assonometrica.

$$T_L = \iint_{As} \tau_{\lim}\cdot dx\cdot dy \quad (10)$$

where A_s is the area of lateral faces P'Q'R' and P'Q'Q' of the wedge and τ_{lim} is the limit shear strength along them, which can be expressed as a function of the normal horizontal stress σ'_{hL} acting perpendicular to the lateral face:

$$\tau_{\lim} = \sigma'_{hL}\cdot\tan\varphi' = K_s\cdot\sigma'_{v}\cdot\tan\varphi' \quad (11)$$

In equation (11), K_s is a lateral earth pressure coefficient relating horizontal and vertical normal effective stresses. Details of the derivation of equation (10) can be found in MOTTA [2012].

Combining equation (7) with equation (8), the expression of the thrust of the plate at limit equilibrium can be obtained:

$$S_{p3D} = \frac{[W\cdot(1-K_v) + 2\cdot T_L\cdot\sin\eta]\cdot\tan(\alpha+\varphi') - k_h\cdot W + 2\cdot T_L\cdot\cos\eta}{\cos\delta - \sin\delta\cdot\tan(\alpha+\varphi')} \quad (12)$$

Substituting in equation (12) explicit values for W and T_L and dividing passive earth pressure S_{p3D} for the quantity $\frac{\gamma\cdot(1-K_v)\cdot H^2}{2} B$, after some simple substitutions, the average passive thrust coefficient for a finite width B of soil mass is obtained:

$$K_{p3D}=\frac{\sin(\alpha+\varphi'-\theta)-n_s\cdot\cos\varepsilon\cdot\tan\varphi'\cdot\cos\theta\cdot\cos(\alpha+\varphi'-\eta)}{\cos\theta\cdot(\tan\alpha-\tan\varepsilon)\cdot\cos(\alpha+\varphi'-\delta)} \quad (13)$$

being:

$$n_s=\frac{2}{3}\cdot\frac{H}{B}\cdot\frac{K_s}{1-K_v} \quad (14)$$

The general equation for the 3D passive earth thrust then becomes:

$$S_{p3D}=\frac{1}{2}\cdot\gamma\cdot(1-K_v)\cdot B\cdot H^2\cdot K_{p3D} \quad (15)$$

In deriving K_{p3D}, the vertical seismic coefficient K_v must be assumed positive if the vertical inertial action acts upwards (Fig. 2).

The critical angle α_c, for which S_{p3D} is minimum, is given by:

$$\alpha_c=\tan^{-1}\left[\frac{-B+\sqrt{B^2-4\cdot A\cdot C}}{2\cdot A}\right] \quad (16)$$

being:

$$A=-\cos\varepsilon\cdot\sin(\varphi'+\delta)\cdot[n_s\cdot\cos\varepsilon\cdot\tan\varphi'\cdot\cdot\cos\theta\cdot\sin(\varphi'-\eta)+\cos(\varphi'-\theta)] \quad (17)$$

$$B=\cos\varepsilon\cdot\{\cos(\delta-\theta)-\cos(2\varphi'+\delta-\theta)-n_s\cdot\cos\varepsilon\cdot\cdot\tan\varphi'\cdot\cos\theta\cdot[\sin(\delta+\eta)+\sin(2\varphi'+\delta-\eta)]\} \quad (18)$$

$$C=\cos\varepsilon\cdot\cos(\varphi'+\delta)\cdot[n_s\cdot\cos\varepsilon\cdot\tan\varphi'\cdot\cos\theta\cdot\cos(\varphi'-\eta)-\sin(\varphi'-\theta)]+\sin\varepsilon\cdot[n_s\cos\varepsilon\cdot\tan\phi'\cdot\cos\theta\cdot\sin(\delta+\eta)-\cos(\delta+\theta)] \quad (19)$$

The three dimensional passive earth pressure coefficient becomes then:

$$K_{p3D}=\frac{\sin(\alpha_c+\varphi'-\theta)-n_s\cdot\cos\varepsilon\cdot\tan\varphi'\cdot\cos\theta\cdot\cos(\alpha_c+\varphi'-\eta)}{\cos\theta\cdot(\tan\alpha_c-\tan\varepsilon)\cdot\cos(\alpha_c+\varphi'+\delta)} \quad (20)$$

Different inclinations, η, of the lateral resistance, T_L, in equation (20) will bring to different K_{p3D} values. For example, in figure 3, K_{p3D} values are plotted versus B/H for two different values of η (η=0 and η=α_c, being α_c the critical angle of equation 16). In the two analyzed cases, δ/ φ'=0 and δ/ φ'=0,5 for the lower values of B/H ratio, K_{p3D} is sensitive to η angle value. Obviously, for high values of B/H, K_{p3D} is no longer influenced by η because the problem is similar to a two-dimensional one.

It is reasonable to assume that the inclination η, of the lateral resistance, T_L, is equal to the angle of failure plain, α_c that is unknown "a priori", so that, for a best estimation of K_{p3D}, an iterative procedure is suggested, whose flow chart is shown in figure 4. Only few iterations are necessary to obtain $|\alpha_c^{(i+1)}-\zeta|<\zeta$, where ξ is the required accuracy.

As said previously, in equation (11), K_s is a lateral earth pressure coefficient relating horizontal and vertical normal stress. Even if its value depends on several factors, such as soil strength, soil deformability, stress history and so on, in a rigid plastic soil behavior, it is reasonable to assume that it should depend significantly on the soil friction angle φ'. It is not the aim of the present paper to investigate on the K_s value. Here just some indications are given on the basis of comparisons with numerical solutions by other authors. For example, figure 5 shows, for the case φ'=30° and δ/ φ'=0, a comparison between values of the three dimensional passive earth pressure coefficient deduced by SOUBRA and REGENASS [2000] and curves deduced by the present model for three different K_s values: the earth pressure coefficient at rest for normally consolidated soils, K_0=1–sin φ', the RANKINE passive earth pressure coefficient, K_p=tan^2 (45° + φ'/2), and the average, K_{AV}, between K_0 and K_p.

A very good agreement between results of equation (15) and those presented by SOUBRA and REGENASS [2000] is found if in equation (14) it is assumed $K_s = K_{AV}$; thus this value has been assumed in the analysis.

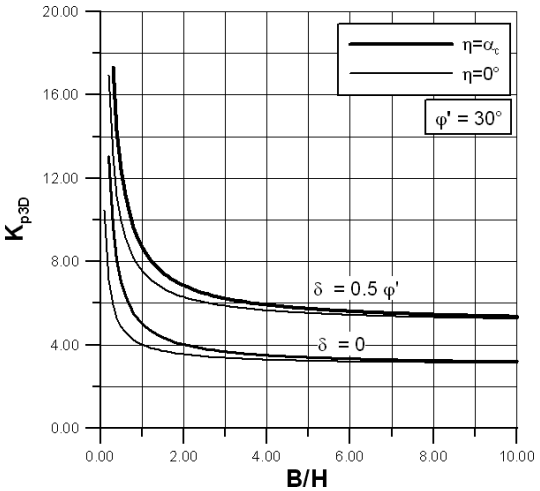

Fig. 3 – K_{p3D} versus B/H for two different values of η, in the case δ/ φ'=0 and e δ/ φ'=0,5.
Fig. 3 – K_{p3D} in funzione di B/H per due diversi valori di η, *nel caso* δ/ φ'*=0 e* δ/ φ'*=0,5.*

4. Comparison of 3D passive earth pressure coefficient with those presented by other authors.

BLUM [1932] first presented a three dimensional solution for the passive earth pressure coefficient, using the limit equilibrium approach. Blum's mechanism is an extension into three dimensions of the traditional one-block Coulomb mechanism in which frictional forces at the lateral planes are neglected. The lower slip surface is assumed to be planar, as in COULOMB [1773] and KAPILA [1962] theories. According to BLUM, the 3D passive earth thrust is given by:

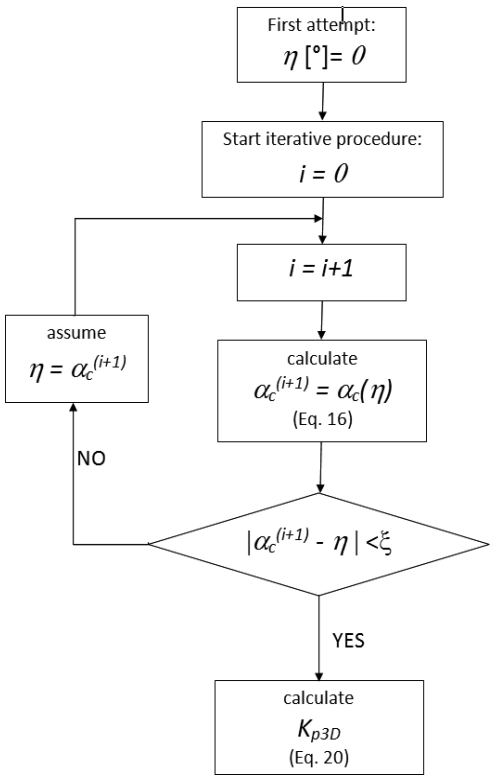

Fig. 4 – Flow chart for the determination of η and K_{p3D}.
Fig. 4 – Diagramma di flusso per la valutazione di η *e* K_{p3D}.

$$S_{p3D} = \frac{1}{2}\cdot\gamma\cdot H^2\cdot B\cdot\tan^2\left(\frac{\pi}{4}+\frac{\varphi'}{2}\right)+\gamma\cdot\frac{H^3}{6}\cdot\tan^2\left(\frac{\pi}{4}+\frac{\varphi'}{2}\right) \quad (21)$$

Blum equation does not take into account the soil-structure interface friction angle (δ=0°), but it has the advantage of giving a closed form solution, which is of some utility in practical engineering.

SOUBRA and REGENASS [2000] investigated the 3D passive earth pressure coefficient by the upper-bound theorem of limit analysis. Three kinematically admissible translational failure mechanisms, referred to as M_1 (One Block Mechanism), M_n (Multiblock Mechanism) and M_{nt} (Truncated Multiblock Mechanism), were considered for the calculation schemes. The authors concluded that the M_{nt} mechanism is the most efficient, and for practical use, they proposed numerical results based on the M_{nt} mechanism for various governing parameters.

In figure 6, for the case δ/φ'=0, solutions by BLUM [1932] (Eq. 21), SOUBRA and REGENASS [2000] for M_{nt} truncated multi-block mechanism and the presented approach (Eq. 20) are shown. For the case φ'=15° there is a very good agreement between the compared three coefficients while for φ'=35° Blum's solution gives results on the safe side, with respect to equation 15, probably for neglecting frictional forces at the lateral planes.

For the cases δ/φ'=0,5 and δ/φ'=1, in figures 7 and 8 respectively, solutions presented by SOUBRA and REGENASS [2000] for M_{nt} truncated multi-block mechanism and the presented approach are shown for φ'=15° and φ'=35°. BLUM's solution cannot be considered because in his model S_{p3D} is assumed acting perpendicularly to the plate and does not take into account the influence of the angle δ. As expected, the proposed model, based on a plane failure surface gives too high values of K_{p3D} in the case δ/φ'=1. However, for all other cases, results obtained by equation (20) are in good agreement with those by SOUBRA and REGENASS [2000].

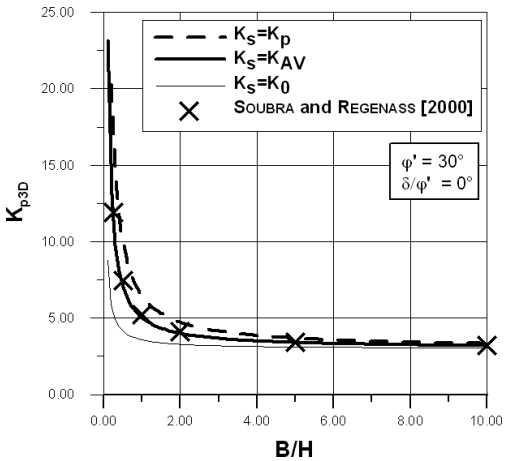

Fig. 5 – K_{p3D} versus B/H for different K_s values, ($K_s = K_0$; $K_s = K_{AV}$; $K_s = K_p$), in the case φ'=30° and δ/ φ'=0.
Fig. 5 – K_{p3D} *in funzione di B/H per differenti valori di* K_s *assegnati (*$K_s = K_0$*;* $K_s = K_{AV}$*;* $K_s = K_p$*), nel caso* φ'*=30° e* δ/ φ'*=0.*

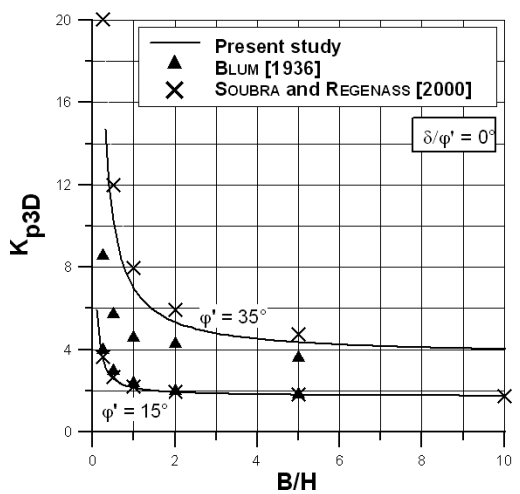

Fig. 6 – K_{p3D} versus B/H in the cases φ'=15° and φ'=35°: comparison between BLUM [1932] solution, SOUBRA and REGENASS [2000] solution and the proposed one (δ/ φ'=0).
Fig. 6 – K_{p3D} *in funzione di B/H nei casi* φ'*=15° e* φ'*=35°: confronto fra la soluzione di BLUM [1932], quella di SOUBRA e REGENASS [2000] e quella proposta (*δ/ φ'*=0).*

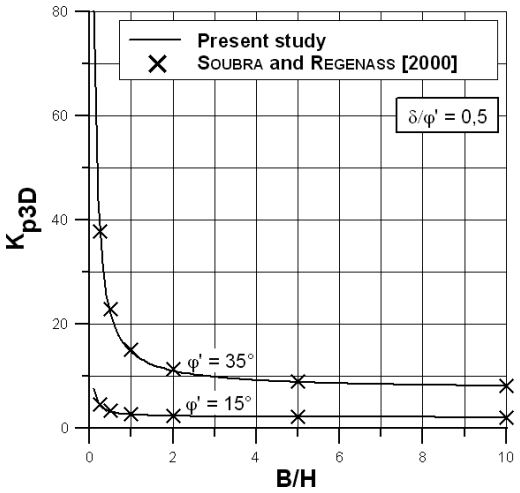

Fig. 7 – K_{p3D} versus B/H in the cases φ'=15° and φ'=35°: comparison between SOUBRA and REGENASS [2000] solution and the proposed one (δ/ φ'=0.5).
Fig. 7 – K_{p3D} in funzione di B/H nei casi φ'=15° and φ'=35°: confronto fra la soluzione di SOUBRA e REGENASS [2000] e quella proposta (δ/ φ'=0.5).

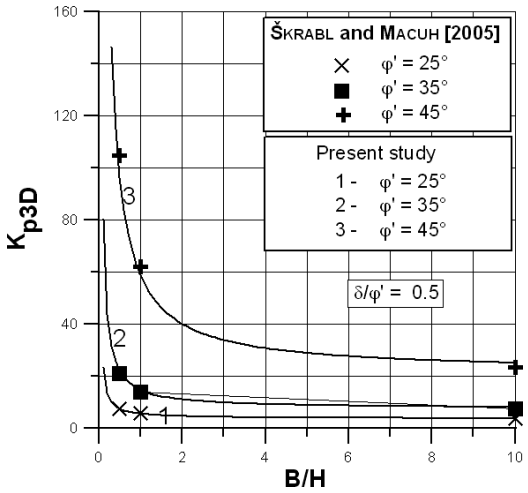

Fig. 9 – K_{p3D} versus B/H in the case δ/ φ'=0,5, for three different values of the friction angle: φ'=25° φ'=35° φ'=45°: comparison between SKRABL and MACHU [2007] solution and the proposed one.
Fig. 9 – K_{p3D} in funzione di B/H nel caso δ/ φ'=0,5, per tre diversi valori dell'angolo di attrito: φ'=25° φ'=35° φ'=45°: confronto fra la soluzione di SKRABL e MACHU [2007] e quella proposta.

Based on the limit analysis theory, SKRABL and MACHU [2005], developed a rotational hyperbolical failure mechanism representing an extension of the plane slip surface in the shape of a log spiral. The outer sides are laterally bounded by a curved and kinematically-admissible hyperbolic surface. Comparison between SKRABL and MACHU [2005] results and the present study, for δ/φ'=0,5 and for three different values of the friction angle (φ'=25°, φ'=35°, φ'=45°), is shown in figure 9. A very good agreement between the two approaches for all the analyzed *B/H* ratio values is obtained.

In the model presented by VRECL-KOJC and SKRABL [2007] a modified three-dimensional (3D) translational failure mechanism was proposed, using the upper bound theorem of the limit analysis theory.

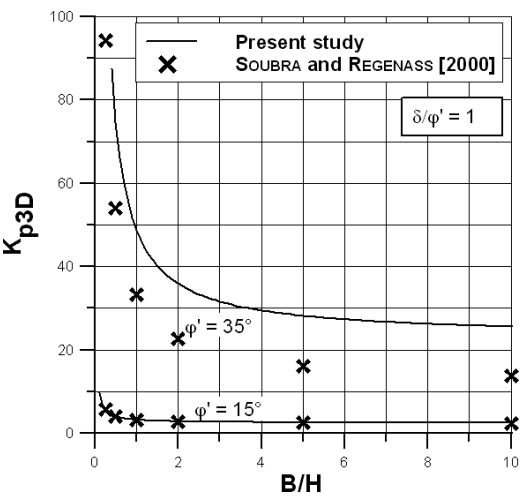

Fig. 8 – K_{p3D} versus B/H in the cases φ'=15° and φ'=35°: comparison between SOUBRA and REGENASS 2000] solution and the proposed one (δ/ φ'=1).
Fig. 8 – Andamento di K_{p3D} nei casi φ'=15° and φ'=35°: confronto fra la soluzione di SOUBRA e REGENASS [2000] e quella proposta (δ/ φ'=1).

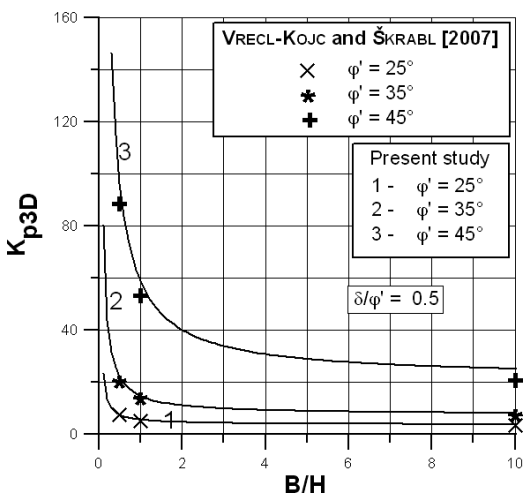

Fig. 10 – K_{p3D} versus B/H in the case δ/ φ'=0,5, for three different values of the friction angle: φ'=25° φ'=35°, φ'=45°: comparison between VRECL-KOJC and SKRABL [2007] solution and the proposed one.
Fig. 10 – K_{p3D} in funzione di B/H nel caso δ/ φ'=0,5, per tre diversi valori dell'angolo di attrito: φ'=25° φ'=35°, φ'=45°: confronto fra la soluzione di VRECL-KOJC e SKRABL [2007] e quella proposta.

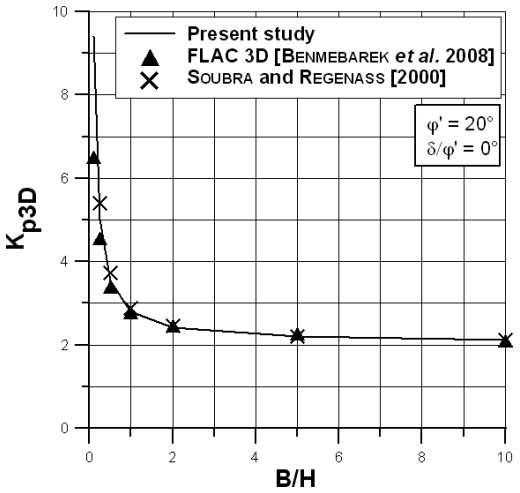

Fig. 11 – Comparison between solutions by BENMEBAREK *et al.* [2008], by SOUBRA and REGENASS [2000] and by the proposed model, in the case δ/ φ'=0 and for φ'=20°.
Fig. 11 – Confronto fra le soluzioni di BENMEBAREK et al. *[2008], di SOUBRA e REGENASS [2000] e quella proposta, nel caso* δ/ φ'*=0, per* φ'*=20°.*

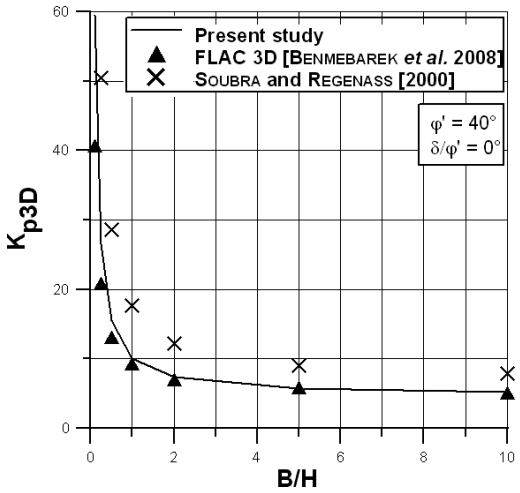

Fig. 13 – Comparison between solutions by BENMEBAREK *et al.* [2008], by SOUBRA and REGENASS [2000] and by the proposed model, in the case δ/ φ'=0 and for φ'=40°.
Fig. 13 – Confronto fra le soluzioni di BENMEBAREK et al. *[2008], di SOUBRA e REGENASS [2000] e quella proposta, nel caso* δ/ φ'*=0, per* φ'*=40°.*

Similarly to figure 9, in figure 10 a comparison between VRECL-KOJC and SKRABL [2007] results for δ/φ'=0,5 and for three different values of the friction angle (φ'=25°, φ'=35°, φ'=45°), is shown. Also in this case, a very good agreement of VRECL-KOJC and SKRABL [2007] results with those given by equation(20) is found for all the analyzed *B/H* ratio values.

Finally, BENMEBAREK *et al.* [2008] carried out a parametric analysis to show the increase of the passive pressures due to the decrease of the retaining wall width. The three-dimensional code FLAC3D, that applies an explicit finite difference approach, was utilized. Figures from 11 to 16 show comparisons between results calculated by equation (20), and numerical results obtained by BENMEBAREK *et al.* [2008] and by SOUBRA and REGENASS [2000] for the cases φ'=20°, φ'=30°, φ'=40° and for a ratio δ/φ'=1/3. We can observe that plots are in a good agreement and values computed by equation (20)

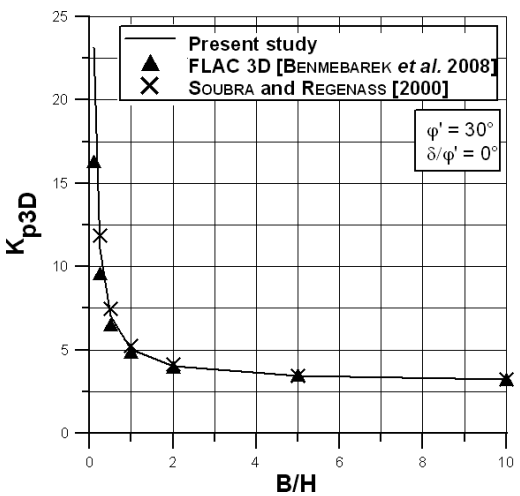

Fig. 12 – Comparison between solutions by BENMEBAREK *et al.* [2008], by SOUBRA and REGENASS [2000] and by the proposed model, in the case δ/ φ'=0 and for φ'=30°.
Fig. 12 – Confronto fra le soluzioni di BENMEBAREK et al. *[2008], di SOUBRA e REGENASS [2000] e quella proposta, nel caso* δ/ φ'*=0, per* φ'*=30°.*

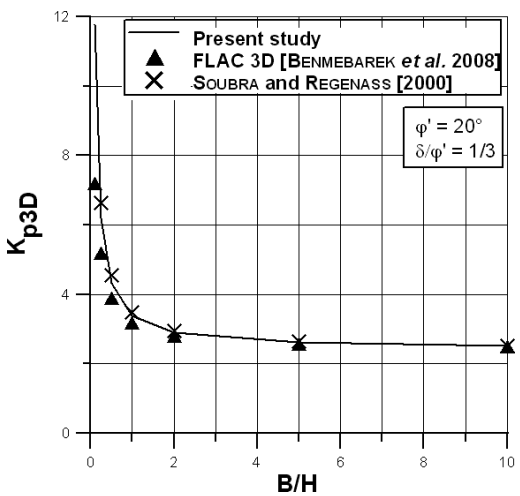

Fig. 14 – Comparison between solutions by BENMEBAREK *et al.* [2008], by SOUBRA and REGENASS [2000] and by the proposed model, in the case δ/ φ'=1/3 and for φ'=20°.
Fig. 14 – Confronto fra le soluzioni di BENMEBAREK et al. *[2008], di SOUBRA e REGENASS [2000] e quella proposta, nel caso* δ/ φ'*=1/3, per* φ'*=20°.*

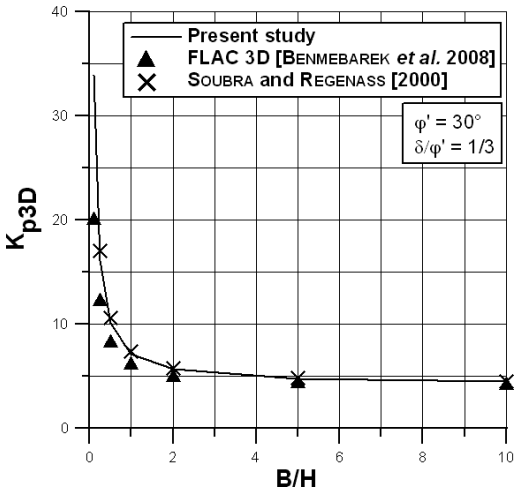

Fig. 15 – Comparison between solutions by BENMEBAREK *et al.* [2008], by SOUBRA and REGENASS [2000] and by the proposed model, in the case δ/ φ'=1/3 and for φ'=30°.
Fig. 15 – Confronto fra le soluzioni di BENMEBAREK et al. *[2008], di SOUBRA e REGENASS [2000] e quella proposta, nel caso* δ/ φ'*=1/3, per* φ'*=30°.*

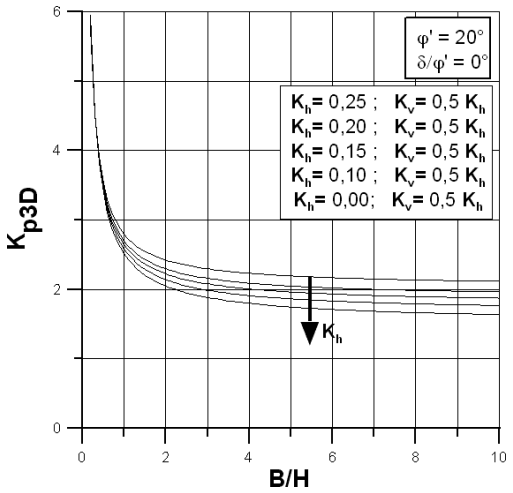

Fig. 17 – Seismic passive earth pressure coefficient K_{p3D} coefficient versus B/H for different seismic horizontal coefficient K_h in the case δ/ φ'=0 and for φ'=20°.
Fig. 17 – Coefficiente di spinta passiva tridimensionale in condizioni sismiche, K_{p3D}, per diversi valori del coefficiente sismico orizzontale K_h nel caso δ/ φ'*=0, per* φ'*=20°.*

are intermediate between SOUBRA and REGENASS [2000] and BENMEBAREK *et al.* [2008].

5. Seismic coefficients and slope angle effects on K_{P3D} values

Differently from numerical approaches presented by other authors in literature, the closed form solution proposed in this paper allows to take into account the effect of seismic coefficients, in a pseudo-static approach and that of the slope angle on K_{p3D} value.

For as regards seismic coefficients, K_h and K_v, as an example, for the case δ=0°, figure 17, 18 and 19 show K_{p3D} versus B/H ratio, for different K_h and K_v values, and for φ=20°, φ=30°, and φ=40°, respectively. In all the analysed cases, the vertical seismic coefficient K_v is assumed the half of the horizontal one, K_h. Differences in K_{p3D} for seismic horizontal coefficients varying from 0 to 0.25 are appreciable only

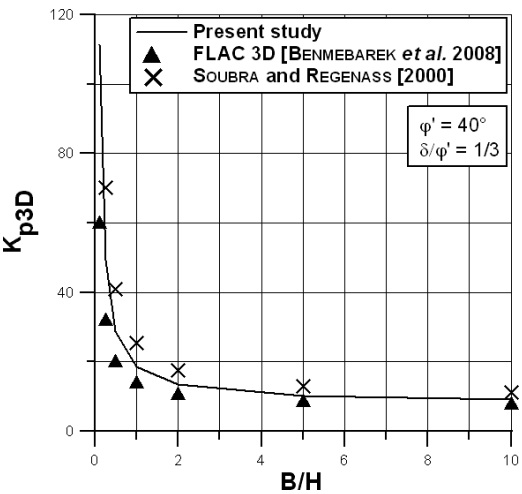

Fig. 16 – Comparison between solutions by BENMEBAREK *et al.* [2008], by SOUBRA and REGENASS [2000] and by the proposed model, in the case δ/ φ'=1/3 and for φ'=40°.
Fig. 16 – Confronto fra le soluzioni di BENMEBAREK et al. *[2008], di SOUBRA e REGENASS [2000] e quella proposta, nel caso* δ/ φ'*=1/3, per* φ'*=40°.*

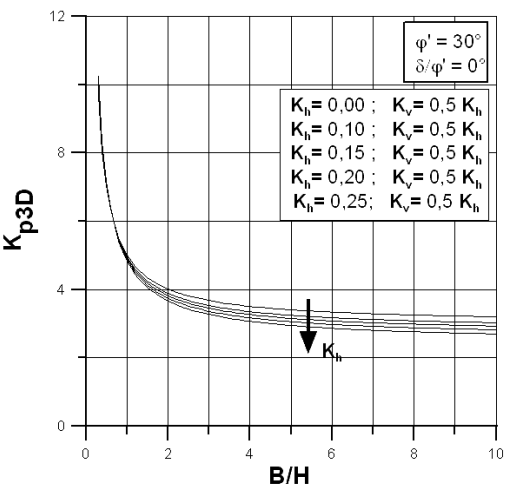

Fig. 18 – Seismic passive earth pressure coefficient K_{p3D} coefficient versus B/H for different seismic horizontal coefficient K_h in the case δ/ φ'=0 and for φ'=30°.
Fig. 18 – Coefficiente di spinta passiva tridimensionale in condizioni sismiche, K_{p3D}, per diversi valori del coefficiente sismico orizzontale K_h nel caso δ/ φ'*=0, per* φ'*=30°.*

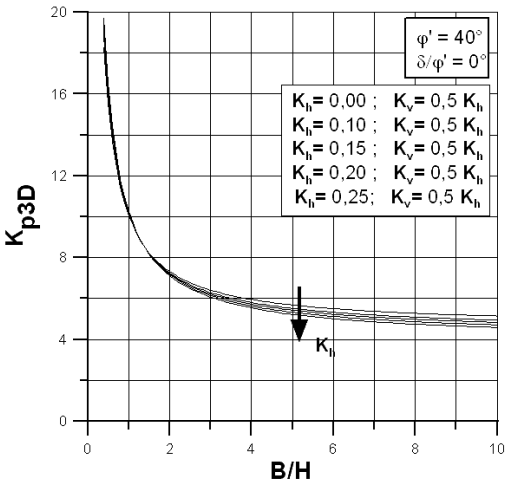

Fig. 19 – Seismic passive earth pressure coefficient K_{p3D} coefficient versus B/H for different seismic horizontal coefficient K_h in the case δ/ φ'=0 and for φ'=40°.

Fig. 19 – Coefficiente di spinta passiva tridimensionale in condizioni sismiche, K_{p3D}, per diversi valori del coefficiente sismico orizzontale K_h nel caso δ/ φ'=0, per φ'=40°.

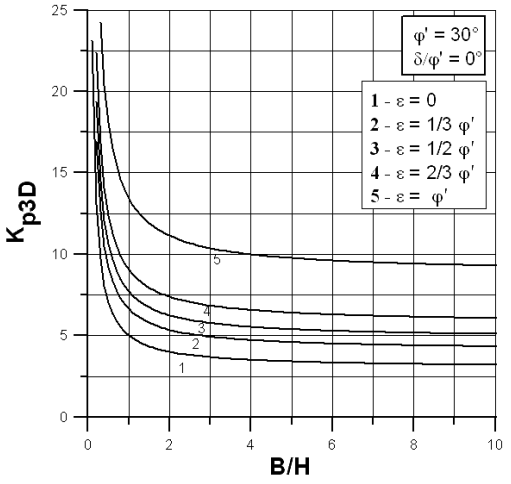

Fig. 21 – Passive earth pressure coefficient K_{p3D} coefficient versus B/H for different slope angles ε, in the case δ/ φ'=0 and for φ'=30°.

Fig. 21 – Coefficiente di spinta passiva tridimensionale, K_{p3D}, per diversi valori dell'angolo di pendio, ε, nel caso δ/ φ'=0, per φ'=30°.

for high values of *B/H*. No great difference is found for low values of *B/H*, because in such cases, inertia forces in the sliding wedge are negligible compared with side effects.

Finally the effect of the slope angle ε on K_{p3D} has been investigated. The angle ε has been assumed ranging from ε=0° to ε= φ'. In figures 20, 21 and 22, values of K_{p3D} computed from equation (20) versus *B/H* ratio have been plotted for the cases φ'=20°, φ'=30°, and φ'=40°. A ratio δ/φ'=0 was assumed. As expected, the higher the slope angle ε, the greater the K_{p3D} values. All the quoted figures show that the effect of ε on K_{p3D} can be very significant. For example for φ'=20° and *B/H* = 0.25, the difference in K_{p3D} values for the cases ε=0 and ε= φ' is about 50% ; moreover, for φ'=40° and *B/H* = 0.25, the difference in K_{p3D} values for the cases ε=0°and ε= φ' is more than 1000% . Thus, the slope of the backfill can affect significantly the static passive thrust. Other applications of the presented model show that this effect is evident also in case of seismic loading, but those results are not presented in this paper.

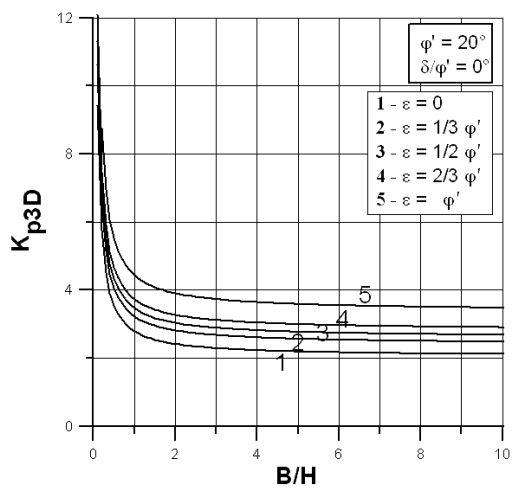

Fig. 20 – Passive earth pressure coefficient K_{p3D} coefficient versus B/H for different slope angles ε, in the case δ/ φ'=0 and for φ'=20°.

Fig. 20 – Coefficiente di spinta passiva tridimensionale, K_{p3D}, per diversi valori dell'angolo di pendio, ε, nel caso δ/ φ'=0, per φ'=20°.

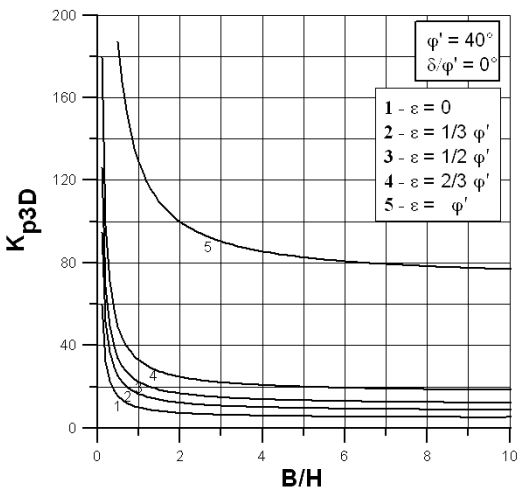

Fig. 22 – Passive earth pressure coefficient K_{p3D} coefficient versus B/H for different slope angles ε, in the case δ/ φ'=0 and for φ'=40°.

Fig. 22 – Coefficiente di spinta passiva tridimensionale, K_{p3D}, per diversi valori dell'angolo di pendio, ε, nel caso δ/ φ'=0, per φ'=40°.

6. Conclusions

An extension of Mononobe-Okabe-Kapila formula has been proposed for the evaluation of a three-dimensional passive earth pressure coefficient, based on the limit equilibrium method. Differently from other studies in literature concerning three-dimensional passive earth pressure, a closed form solution has been provided. For the static case a good agreement was found comparing the proposed solution with results obtained by other authors who used more rigorous approaches such as upper bound solutions of limit analysis. It has been observed that, as expected, the proposed model, based on a plane failure surface, overestimates K_{p3D} values for higher δ/φ' ratios. Moreover, similarly than in Mononobe-Okabe-Kapila formula, the presented solution allows to take into account, in a pseudo static approach, the effects of inertia forces due to earthquakes, so it can be used for seismic design in all the cases where a dynamic passive earth pressure must be considered. Equation (20) also allows the angle of the soil slope to be considered in the evaluation of passive earth pressure coefficient. This can be of great utility considering that the slope of the backfill can affect significantly the static and/or the seismic passive thrust.

References

Benmebarek S., Khelifa T., Benmebarek N., Kastner R. (2008) – *Numerical evaluation of 3D passive earth pressure coefficients for retaining wall subjected to translation.* - Computers and Geotechnics, 35, pp. 47-60.

Benmeddour D., Mellas M., Mabrouki A. (2010) – *Étude numerique des pressions passives appliquées sur un bloc d'ancrage rigide.* - Courrier du Savoir, n. 10, pp. 43-49 (in French).

Blum H. (1932) – *Wirtschaftliche Dalbenformen und deren Berechnung.* Bautechnik, 10, n. 5, pp. 122-135 (in German).

Caquot A., Kerisel J. (1949) – *Traité de mécanique des sols* - Gauthier-Villars, Paris (in French).

Chen W. F., Rosenfarb J.L. (1973) – *Limit analysis solutions of earth pressure problems.* - Soils and Foundations, Tokyo, 13, n. 4, pp. 45-60.

Coulomb C.A. (1773) – *Essai sur une application des règles de maximis et minimis à quelques problèmes de statique relatifs à l'architecture.* - ACAD. r.Sci. Memoires de l'Académie Royale Math. Phys. par divers savants, 7, pp. 343-382 (in French).

Kapila J. P. (1962) – *Earthquake Resistant Design of Retaining Walls.* - Proc. 2nd Earthquake Symposium, University of Roorkee, Roorkee, India.

Lancellotta R. (2002) – *Analytical solution of passive earth pressure.* Géotechnique, vol. LII, n. 8, pp. 617-619.

Lancellotta R. (2007) – *Lower-Bound approach for seismic passive earth resistance.* Géotechnique, 57, n. 3, pp. 319-321.

Lee I. K., Herington J. R. (1972) – *A theoretical study of the pressures acting on a rigid wall by a sloping earth on rockfill.* Géotechnique, 22, n. 1, pp. 1-26.

Lysmer J. (1970) – *Limit analysis of plane problems in soil mechanics.* Journal for Soil Mechanics and Foundation Division, ASCE, 96, n. 4, pp. 1311-1334.

Mononobe N., Matsuo H. (1929) – *On the determination of earth pressures during earthquakes.* Proc. World Engineering Conference, vol. IX, pp. 176.

Motta E. (1994) – *Generalized Coulomb Active Earth Pressure for Distanced Surcharge.* Journal of Geotechnical Engineering, 120, n. 6, June 1994 , pp. 1072-1079.

Motta E. (2012) – *Sul coefficiente di spinta attiva in terrapieni di lunghezza finita.* Italian Geotechnical Journal, n. 4, pp. 57-65.

Okabe S. (1926) – *General theory of earth pressure*, Journal of Japanese Society of Civil Engineering, vol. XII, n. 1.

Rahardjo H., Fredlund D.G. (1984) – *General limit equilibrium method for lateral earth force.* Canadian Geotechnical Journal, Ottawa, 21, n. 1, pp. 166-175.

Rankine W. (1857) – *On the stability of loose earth.*- Philosophical Transactions of the Royal Society of London, vol. CXLVII.

Shields D.H., Tolunay A.Z. (1973) – *Passive pressure coefficients by methods of slices.* Journal of Soil Mechanics and Foundation Division, ASCE, 99, n. 12, pp. 1043-1053.

Sokolovski V.V. (1960) – *Static of soil media.* Butterworth's scientific publications, London, 237 pp.

Soubra A.H. (2000) – *Static and seismic passive earth pressure coefficients on rigid retaining structures.* Canadian Geotechnical Journal, 37, n. 2, pp. 463-478.

Soubra A.H., Macuh B. (2002) – *Active and passive earth pressure coefficients by a kinematical approach.* Proceedings of the Institution of Civil Engineers Geotechnical Engineering, 155, n. 2, pp. 119-131.

Soubra A.H., Regenass P. (2000) – *Three dimensional passive earth pressures by kinematical approach.* Journal of Geotechnical and Geoenvironmental Engineering, ASCE, 2, n. 2, pp. 969-978.

Škrabl S., Macuh B. (2005) – *Upper-bound solutions of three-dimensional passive earth pressures.* Canadian Geotechnical Journal, 42, n. 5, pp. 1449-1460.

Subba Rao K.S., Choudhury D. (2005) – *Seismic passive earth pressures in soils.* Journal of Geotechnical and Geoenvironmental Engineering, ASCE, 131, n. 1, pp. 131-135.

Vrecl-Kojc H., Škrabl S. (2007) – *Determination of passive earth pressure using three dimensional failure mechanism.* Acta Geotechnica Slovenica, 4, n. 1, pp. 10-23.

Zakerzadeh N., Fredlund D.G., Pufahl D.E. (1999) – *Interslice force functions for computing active and passive earth force.* Canadian Geotechnical Journal, Ottawa, 36, n. 6, pp. 1015-1029.

List of Symbols

B = plate width
H = plate height
K_h = horizontal seismic coefficient
K_v = vertical seismic coefficient
θ = seismic angle
K_{PE} = two-dimensional dynamic passive earth pressure coefficient
φ' = soil friction angle
β = inclination of the plate interior side
δ = soil-plate interface friction angle
ε = backfill slope angle
α_{PE} = inclination of the critical failure surface in Mononobe-Okabe-Kapila method.
α_c = inclination of the critical failure surface in the presented method.
ξ = required accuracy for the iterative procedure suggested to obtain η angle.
T_B = base resistance of the failure wedge;
T_L = lateral resistance acting of each side of the failure wedge
N' = normal force on the base of the failure wedge
η = angle of T_L with respect to the horizontal direction
S_{p3D} = three dimensional passive earth pressure
K_{p3D} = three dimensional passive earth pressure coefficient
A_s = area of lateral faces of the wedge
W = weight of the wedge
K_0 = earth pressure coefficient at rest for normally consolidated soils
K_p = Rankine passive earth pressure coefficient
K_{AV} = average value between K_0 and K_p.

Una soluzione in forma chiusa per il coefficiente di spinta passiva tridimensionale

Sommario

La valutazione della spinta passiva, sia in condizioni statiche sia in condizioni sismiche, è molto importante per la progettazione di paratie, ancoraggi, fondazioni, ecc. Nella letteratura tecnica è stato dimostrato che, nel caso in cui la piastra sulla quale è applicata la spinta abbia larghezza limitata, l'influenza della terza dimensione può risultare significativa, a causa degli effetti di bordo, così che il coefficiente di spinta passiva tridimensionale risulta maggiore di quello bidimensionale. Purtroppo, allo stato attuale, non è disponibile in letteratura alcuna soluzione in forma chiusa per il calcolo di questo coefficiente, ma solo tabelle o grafici che ne riportano i valori in funzione del rapporto B/H, essendo B ed H , rispettivamente, la larghezza e l'altezza della piastra.

In questo lavoro si presenta un'estensione del classico metodo di MONONOBE-OKABE-KAPILA e si ottiene una soluzione in forma chiusa per il calcolo del coefficiente di spinta passiva tridimensionale, che viene poi applicato. Analogamente agli approcci numerici presenti in letteratura, la soluzione proposta prende in considerazione l'angolo di attrito del terreno e l'angolo di attrito all'interfaccia fra la piastra e il terreno, mentre, come valore aggiunto, consente di considerare l'effetto della pendenza del terrapieno e quello delle azioni sismiche, secondo un approccio pseudo-statico. Il modello viene validato in condizioni statiche, mediante il confronto con soluzioni ottenute da altri autori con approcci differenti.